Available online at www.sciencedirect.com

ScienceDirect

J Materiomics 2 (2016) 265–272

www.ceramsoc.com/en/

www.journals.elsevier.com/journal-of-materiomics/

Improved electrochemical performance of 5 V spinel $LiNi_{0.5}Mn_{1.5}O_4$ microspheres by F-doping and Li_4SiO_4 coating

Ya-Hui Xu [a,b], Shi-Xi Zhao [a,*], Yu-Feng Deng [a,b], Hui Deng [a,b], Ce-Wen Nan [b]

[a] *Graduate School at Shenzhen, Tsinghua University, Shenzhen 518055, China*
[b] *School of Materials Science and Engineering, Tsinghua University, Beijing 100084, China*

Received 22 December 2015; revised 6 April 2016; accepted 7 April 2016
Available online 22 April 2016

Abstract

Porous spinel $LiNi_{0.5}Mn_{1.5}O_4$ microspheres were synthesized by a co-precipitation method. F-doping and Li_4SiO_4-coating were used as two effective ways to enhance the electrochemical performance of $LiNi_{0.5}Mn_{1.5}O_4$ at both room temperature and elevated temperature. All the samples were characterized by thermogravimetric analysis/differential scanning calorimetry (TG/DSC), X-ray diffraction (XRD), inductive coupled plasma-atomic emission spectroscopy (ICP-AES), Raman spectroscopy, scanning electron microscopy (SEM), transmission electron microscopy (TEM) and electrochemical tests, respectively. According to the SEM images, the $LiNi_{0.5}Mn_{1.5}O_4$ microspheres are hollow with porous shell, and each microsphere is made up of nano-sized spinel grains. This hollow and porous structure favors the sufficient contact between electrolyte and the cathode material. It is indicated that 2 wt.% Li_4SiO_4-coated $LiNi_{0.5}Mn_{1.5}O_{3.98}F_{0.02}$ exhibits more superior performance than the pristine one. The doped fluorine ions that enhance the bonding can stabilize the structure of cathode material. The Li_4SiO_4 coating can suppress side reactions between electrolyte and cathode material as a protective material, and it is a superionic conductor with a three-dimensional lithium ion transfer network to decrease the charge-transfer resistance. The discharge capacity retention of 2 wt.% Li_4SiO_4-coated $LiNi_{0.5}Mn_{1.5}O_{3.98}F_{0.02}$ is 97.8% at 25 °C and 94.2% at 55 °C after 150 cycles, respectively.

Keywords: Lithium-ion batteries; Cathode material $LiNi_{0.5}Mn_{1.5}O_4$; Microspheres; F-doping; Li_4SiO_4 coating

1. Introduction

The application targets of lithium ion batteries (LIBs) have evolved from portable electronics devices (i.e., laptops, smart phones and watches) to large-scale applications such as electric vehicles (EVs), hybrid electric vehicles (HEVs) and stationary energy storage wells. To develop the new generation of EVs and HEVs, the batteries require cathode materials that possess both a high energy and a high power for a long cycle life [1,2]. Recent attentions have focused on $LiNi_{0.5}Mn_{1.5}O_4$ as a promising cathode material for LIBs due to its high operating voltage plateau at 4.7 V resulting from $Ni^{2+/4+}$ redox couple, robust close-packed crystal structure, 3D lithium-ion diffusion pathways and relatively benign constituent elements [3]. $LiNi_{0.5}Mn_{1.5}O_4$ has been thus developed for the next generation of high-power batteries.

It is theoretically possible to obtain a perfectly ordered structure with a space group of $P4_332$ in which all Ni^{2+} ions are fully coordinated by six Mn^{4+} nearest-neighbors in the lattice at the Mn:Ni ratio of 3:1. However, it is also theoretically possible to obtain a disordered structure with a space group of $Fd\bar{3}m$ in which Ni^{2+} and Mn^{4+} are distributed randomly among the 16d octahedral sites [4]. The disordered structure exhibits a slight oxygen nonstoichiometry, which is commonly compensated in the presence of a small amount of Mn^{3+} [5]. Usually, a few Mn^{3+} ions arising from oxygen vacancies exist in the structure of $LiNi_{0.5}Mn_{1.5}O_{4-\delta}$, resulting in another voltage plateau at 4.0 V corresponding to Mn^{3+}/

* Corresponding author.
E-mail address: zhaosx@sz.tsinghua.edu.cn (S.-X. Zhao).
Peer review under responsibility of The Chinese Ceramic Society.

http://dx.doi.org/10.1016/j.jmat.2016.04.005

Mn^{4+}. It was believed that the presence of Mn^{3+} could favor the improvement of Li^+-ion transport coefficient as well as the electrical conductivity [6].

At a high discharge voltage plateau of ~4.7 V, $LiNi_{0.5}Mn_{1.5}O_4$ offers a high energy density (~650 W h kg^{-1}), exacerbating undesired side reactions between the active cathode material and the electrolyte solution [7–9]. This can lead to a considerable thickening of the protective solid-electrolyte interphase (SEI) layer passivating on the surface, which is harmful to lithium-ion diffusion [10]. Cations and/or anions doping is considered as an effective way to enhance the performance of $LiNi_{0.5}Mn_{1.5}O_4$. Many doping cations such as Co [11], Ru [12], Fe [13], Zn [14], Mg [15], and Cr [16], which can improve the cyclability, are used to partially substitute Mn and/or Ni. Doping anions such as F [17], S [18] and Cl [19], are used to partially substitute O. It is noticed that a small amount of fluorine substitution improves the electrochemical properties and thermal stability of $LiNi_{0.5}Mn_{1.5}O_4$ [20]. Besides, some studies demonstrated that the surface modification is another effective way to improve the performance of $LiNi_{0.5}Mn_{1.5}O_4$. ZnO [21], ZrO_2 [22], Al_2O_3 [23], BiOF [24], and $AlPO_4$ [25] can be coated on the surface of $LiNi_{0.5}Mn_{1.5}O_4$. These coating materials can protect the active material from HF attack and effectively suppress the occurrence of side reactions, especially at elevated temperatures. However, most of these coating materials are inferior conductors and may impede the Li^+ intercalating or deintercalating, reducing the rate capability. Many researchers [26–28] reported that spinel $LiMn_2O_4$ coated by lithium-ion solid-state electrolytes with a high ion conductivity exhibits a better performance. Since Li_2SiO_3 has a high Li^+-ion conductivity, it can be used to coat on the surface of $LiCoO_2$ [29] and lithium-rich $Li_{1.13}Ni_{0.3}Mn_{0.57}O_2$ [30], acting as a protective layer without blocking the diffusion of Li^+-ion through the layer. Compared to Li_2SiO_3, Li_4SiO_4 as a superionic conductor has the similar structure as Li_2SiO_3, in which the SiO_4 tetrahedra form zigzag chains and lithium ions lay between them forming a three-dimensional network, which contributes to the fast diffusion of Li^+-ion. The difference between Li_4SiO_4 and Li_2SiO_3 is that there are more Li^+-ions existing in the structure of Li_4SiO_4, which are beneficial to the enhancement of capacity and the diffusion of Li^+-ion [31–33]. It is known that the amorphous Li_4SiO_4 film has a high lithium ion conductivity (1.2×10^{-8} S cm^{-1}) [34] and a high electronic conductivity (3.36×10^{-6} S cm^{-1}) [35]. Moreover, Li_4SiO_4 can absorb and digest the traces of HF in the electrolyte, averting the erosion of HF for cathode materials. To our knowledge, little work on the surface modification of the 5 V spinel cathodes with Li_4SiO_4 has been reported.

In this paper, spherical spinel particles of $LiNi_{0.5}Mn_{1.5}O_4$ were synthesized by a carbonate co-precipitation method, which is suitable for industrial production. In addition, F doping and Li_4SiO_4 coating were utilized for the internal and external modifications of $LiNi_{0.5}Mn_{1.5}O_4$ particles to improve the performance. Recently, some novel methods were reported in Refs. [36,37], and the performance of resultant is better, but these methods are not suitable for large-scale preparation.

2. Experimental

2.1. Synthesis of $LiNi_{0.5}Mn_{1.5}O_{4-x}F_x$ microspheres

$LiNi_{0.5}Mn_{1.5}O_{4-x}F_x$ ($x = 0$, 0.02) microspheres were synthesized using spherical $(Ni_{0.25}Mn_{0.75})CO_3$ as a precursor. The stoichiometric amounts of $NiSO_4$ and $MnSO_4$ (1:3) were dissolved in distilled water to prepare a mixed-metal solution A. Na_2CO_3 and $NH_3 \cdot H_2O$ solutions were also separately added to solution A. The pH value of the mixed solution was kept at 8 *via* adding NH_4OH. The reaction was carried out at 55 °C for 3 h. The precipitate was filtered and washed with distill water to remove Na^+ and SO_4^{2-} ions, and then dried at 120 °C and calcined in air at 650 °C for 3 h to obtain the precursor. Afterward, the calcined precursor oxide was mixed with $LiNO_3$ and LiF in ethanol, so that microsphere could not be destroyed. The mixture was evaporated and calcined in air at 850 °C for 10 h.

2.2. Spherical spinel particles coated with Li_4SiO_4

The Li_4SiO_4 solution for surface coating was prepared by a sol–gel method. The stoichiometric amounts of $LiCH_3COO$ and $Si(OC_2H_5)_4$ were dissolved in ethanol. The solution was placed for two days to form Li_4SiO_4 sol solution. The spherical $LiNi_{0.5}Mn_{1.5}O_{4-x}F_x$ sample was added to Li_4SiO_4 sol solution. The mixture was stirred and gently heated to 60 °C until the solvent was evaporated completely. The mixture was heated at 650 °C for 3 h. The weight percentages of the coating material Li_4SiO_4 to the $LiNi_{0.5}Mn_{1.5}O_{4-x}F_x$ particles were 1 wt.%, 2 wt.% and 3 wt.%.

2.3. Characterization

The crystalline phases of the samples were characterized by a model Rint-2000V/PC X-ray diffractometer (XRD, Rigaku, Japan) using Cu Kα radiation at room temperature in the range of 10–70°. The thermal analysis of the samples were performed to detect the weight loss/gain and the reaction processes during the heating of the $(Ni_{0.25}Mn_{0.75})CO_3$ precursors in air at 5 °C/min from 30 °C to 1000 °C by a model STA 449F3 TG/DTA instrument (NETZSCH, Germany). The elementary compositions of the materials were determined by an inductive coupled plasma-atomic emission spectroscope (ICP-AES). Raman spectra were recorded with a model lab-RAM HR800 spectroscope using 532 incident radiation. The morphology of the obtained powders was observed by a model S-4800 field emission scanning electron microscope (SEM, Hitachi, Japan) equipped with an energy dispersive spectrometer (EDS) for elemental analysis, and a model Tecnai G2 F30 transmission electron microscope (TEM, FEI).

2.4. Electrochemical measurements

Electrochemical test was performed with CR2032 coin half-cells composed of the spinel cathode and metallic-lithium anode. Electrolyte for a high-voltage system (~5.0 V vs. Li/

Li^+) was used, the main composition of the electrolyte is 1.1 M LiPF6 in ethylene carbonate (EC)–dimethyl carbonate (DEC) mixture (3:7 ratio by volume) with 1.0 wt.% high voltage additive (Shenzhen CAPCHEM Technology Co. Ltd., China). To prepare the cathodes, the mixture slurry, which contained 80 wt.% cathode materials, 10 wt% acetylene black and 10 wt.% polyvinylidene fluoride (PVDF) in N-methyl-pyrrolidone (NMP), was coated onto an aluminum foil and dried in a vacuum oven at 120 °C for 10 h. All the cells were assembled in an argon-filled glove box. The charge–discharge cycling of the cells was carried out galvanostatically at different current rates, temperatures (25–55 °C) and voltages (3.5–5.0 V) using a model LAND CT2001A battery tester (China).

3. Results and discussion

Fig. 1 shows the TG/DSC curve of the nickel-manganese carbonate precursor. From the DSC curve, the mass of the precursor does not change at 550–750 °C, indicating that no chemical reaction occurs at 550–750 °C. The calcination temperature of the precursor used is thus 650 °C.

Fig. 2 shows the XRD patterns of the product of nickel-manganese carbonate calcined at 650 °C. Two phases are detected in the product, corresponding to Mn_2O_3 and $MnNiO_3$, respectively. The result reveals that the product of nickel-manganese carbonate calcined at 650 °C for 3 h in air is $Mn_2O_3 \cdot MnNiO_3$. As a result, the chemical formula of the product of nickel-manganese carbonate calcined at 650 °C can be determined and the amount of lithium can be controlled accurately in the material. $(Ni_{0.25}Mn_{0.75})CO_3$ precipitate and $LiNi_{0.5}Mn_{1.5}O_4$ are detected by ICP to determine the elementary composition. The result of ICP test confirms the Ni/Mn molar ratio of nickel-manganese carbonate is 0.49:1.51, and the Li:Ni:Mn molar ratio of $LiNi_{0.5}Mn_{1.5}O_4$ is 1.02:0.49:1.51. This implies the co-precipitation reaction is complete, and achieves the purpose of precise control of Li/M mole ratio by nickel-manganese carbonate precursor calcined.

Fig. 3 shows the XRD patterns of the pristine $LiNi_{0.5}Mn_{1.5}O_4$ (LNMO), $LiNi_{0.5}Mn_{1.5}O_{3.98}F_{0.02}$ (LNMOF), 1.0 wt.% Li_4SiO_4-coated $LiNi_{0.5}Mn_{1.5}O_{3.98}F_{0.02}$ (LNMOF-LSO-1), 2.0 wt.% Li_4SiO_4-coated $LiNi_{0.5}Mn_{1.5}O_{3.98}F_{0.02}$ (LNMOF-LSO-2), 3.0 wt.% Li_4SiO_4-coated $LiNi_{0.5}Mn_{1.5}O_{3.98}F_{0.02}$ (LNMOF-LSO-3), respectively. Clearly, all the patterns of five samples can be indexed to well-crystallized cubic spinel $LiNi_{0.5}Mn_{1.5}O_4$ (JCPDS card No.: 80-2162, space group: $Fd\bar{3}m$, $a = 8.170$ Å) without any impurities such as NiO and Li_xNi_yO. The result means the experimental method used is feasible. Anion doping and surface coating do not change the structure obviously. The lattice constants of the five samples are 8.1749 Å, 8.1747 Å, 8.1745 Å, 8.1746 Å, and 8.1748 Å, respectively. The lattice constants of LNMO and LNMOF are similar. Fluoride appears as the most favored dopant and substituent in oxides, because fluoride ionic radius (F^-: 1.33 Å) is similar to the oxygen ionic radius (O^{2-}: 1.32 Å). The energy of Mn–F bond is greater than that of Mn–O bond, which increases the strength of crystal structure. It is conducive to ensure the structure stability of spinel cathode material during the charge and discharge cycle [38].

Fig. 4 shows the Raman spectra of the pristine $LiNi_{0.5}Mn_{1.5}O_4$ (LNMO), $LiNi_{0.5}Mn_{1.5}O_{3.98}F_{0.02}$ (LNMOF),

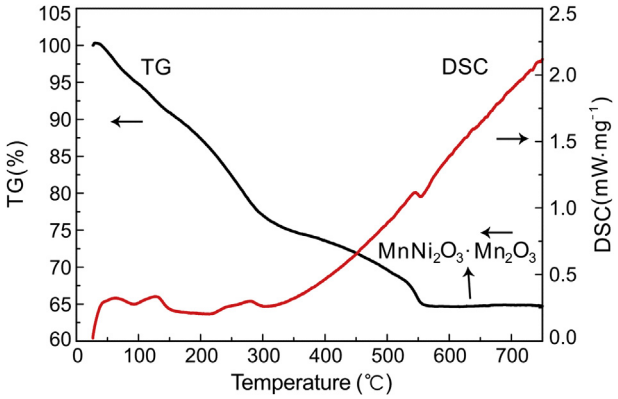

Fig. 1. TG/DSC curves of the nickel-manganese carbonate precursor.

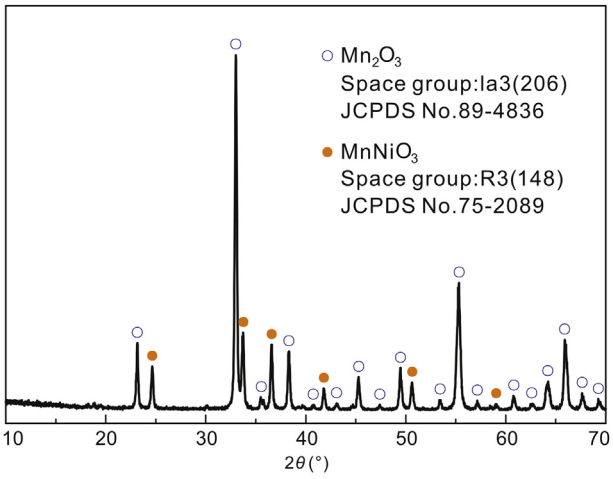

Fig. 2. XRD pattern of the product of $(Ni_{0.25}Mn_{0.75})CO_3$ calcined at 650 °C.

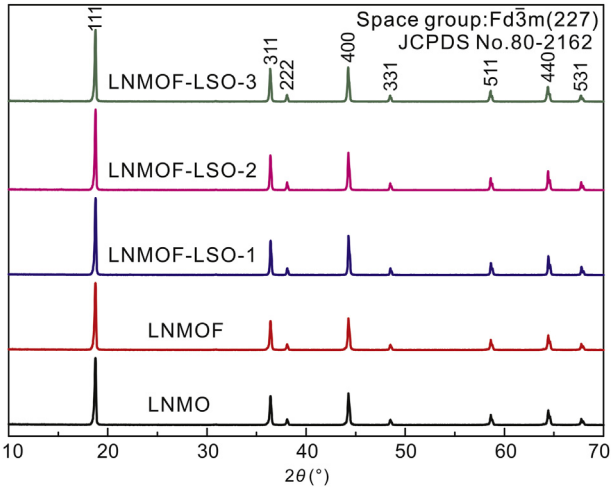

Fig. 3. XRD patterns of the five $LiNi_{0.5}Mn_{1.5}O_4$ samples.

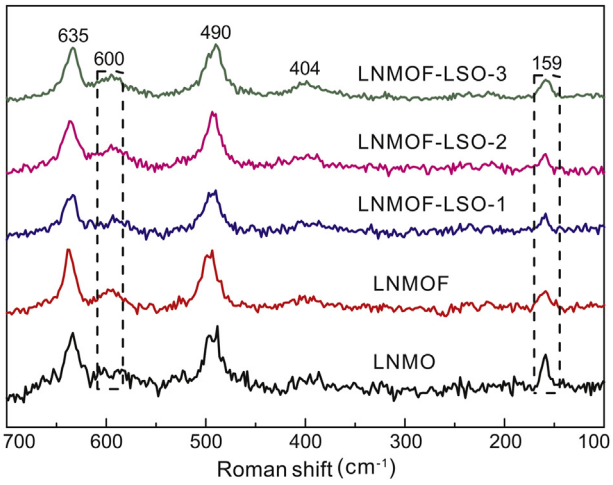

Fig. 4. Raman spectra of the five $LiNi_{0.5}Mn_{1.5}O_4$ samples.

1.0 wt.% Li_4SiO_4-coated $LiNi_{0.5}Mn_{1.5}O_{3.98}F_{0.02}$ (LNMOF-LSO-1), 2.0 wt.% Li_4SiO_4-coated $LiNi_{0.5}Mn_{1.5}O_{3.98}F_{0.02}$ (LNMOF-LSO-2), 3.0 wt.% Li_4SiO_4-coated $LiNi_{0.5}Mn_{1.5}O_{3.98}F_{0.02}$ (LNMOF-LSO-3), respectively. The number of expected Raman-active modes in the ordered spinel (6A1 + 14E + 22F2) is greater than that in the disordered spinel (Ag + Eg+3F2 g) [39]. The intense peaks at 635 cm^{-1} are assigned to the symmetric Mn−O stretching vibration of MO_6 groups, belonging to Ag mode. The peaks at 490 and 404 cm^{-1} are assigned to the Ni^{2+}−O stretching mode in the structure. The splitting of peaks in the 588−623 cm^{-1} region is characteristic of the ordered structure ($P4_332$). Also, the weak bands at 159 cm^{-1} are the features of $P4_332$ structure [40,41]. The peaks of LNMOF sample and coated LNMOF samples do not split, compared to the pristine one, and the peak at 159 cm^{-1} of LNMOF is weaker than that of LNMO, demonstrating that the doped F enhances the degree of cation disordering resulting from more Mn^{3+} ions. Moreover, the doped F exists in the crystal lattice and leads to the increase of Mn^{3+} ions.

Fig. 5 shows the SEM images of precursor $(Ni_{0.25}Mn_{0.75})CO_3$, the intermediate product $Mn_2O_3{\cdot}MnNiO_3$ and spinel $LiNi_{0.5}Mn_{1.5}O_4$. In Fig. 5a and b, the morphology of $(Ni_{0.25}Mn_{0.75})CO_3$ precursor appears spherical. The morphologies of $Mn_2O_3{\cdot}MnNiO_3$ (see Fig. 5c and d), and $LiNi_{0.5}Mn_{1.5}O_4$ (see Fig. 5e and f) remain spherical. Fig. 5g shows the SEM image of the cross-section of $LiNi_{0.5}Mn_{1.5}O_4$ sphere. Compared to $(Ni_{0.25}Mn_{0.75})CO_3$ and $Mn_2O_3{\cdot}MnNiO_3$, $LiNi_{0.5}Mn_{1.5}O_4$ has a complete crystallinity. In Fig. 5e–g, there are some pores on the surface and the microspheres are hollow. The special structure is beneficial to the infiltration of electrolyte and the increase of the contact area between the particles and the electrolyte, which results in the improvement of the rate capability of the material.

Fig. 6 shows the SEM and TEM images of LNMO and LNMOF-LSO-2 samples. In Fig. 6b and d, Li_4SiO_4 evenly distributes on the surface of the LNMOF, compared to the uncoated LNMO (see Fig. 6a and c). The coating of Li_4SiO_4

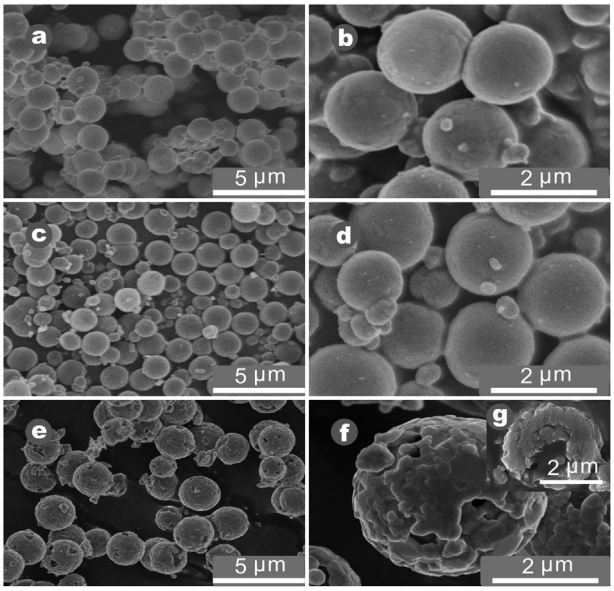

Fig. 5. SEM images of the $(Ni_{0.25}Mn_{0.75})CO_3$, $3Mn_2O_3{\cdot}2NiO$, and LNMO samples: (a and b) $(Ni_{0.25}Mn_{0.75})CO_3$; (c and d) $3Mn_2O_3{\cdot}2NiO$; (e, f and g (cross-section)) LNMO.

appears amorphous, the thickness is about 4–7 nm (see Fig. 6d). Fig. 7 shows the EDS pattern and electron probe micro-analysis images for Mn, Ni and Si elements of LNMOF-LSO-2 sample. A large amount of carbon results from carbon-rich conductive plastic on which the sample is adhered. The EDS results also reveal even distribution of Si on the surface of the particles, consistent with the SEM and TEM images.

Fig. 8a shows the typical galvanostatic charge–discharge curves of the five samples under 0.1 C at 25 °C. The five samples show the similar charge and discharge curves in 4.7 V and 4 V voltage platforms, which are ascribed to Ni^{2+}/Ni^{4+} and Mn^{3+}/Mn^{4+}, respectively. The structure and intrinsic charge–discharge mechanism of $LiNi_{0.5}Mn_{1.5}O_4$ are not changed by doping F and coating Li_4SiO_4. Compared to the pristine spinel $LiNi_{0.5}Mn_{1.5}O_4$ (138 mA h g^{-1}), the initial discharge-specific capacity and 4 V voltage platform of $LiNi_{0.5}Mn_{1.5}O_{3.98}F_{0.02}$ (140.3 mA h g^{-1}) increases slightly due to the higher amount of Mn^{3+} in LNMOF. The 4.0 V plateau of the pristine spinal $LiNi_{0.5}Mn_{1.5}O_4$ is shorter than that of the other four samples, demonstrating that doped F causes the increase of the amount of Mn^{3+}. Moreover, the Li_4SiO_4 coating contributes to the initial discharge-specific capacity with the increase of LNMOF-LSO-1 (141.7 mA h g^{-1}), LNMOF-LSO-2 (142.5 mA h g^{-1}) and LNMOF-LSO-3 (143 mA h g^{-1}). The initial discharge-specific capacity increases slightly with the increment of the amount of coating due to the increment of lithium ion in the coating layer.

Fig. 8b and d shows the cycling curves of LNMO, LNMOF, LNMOF-LSO-1, LNMOF-LSO-2 and LNMOF-LSO-3 under 5 C charge–discharge rate in the voltage range of 3.5–5.0 V at 25 °C and 55 °C, respectively. The initial discharge capacities of the five samples at 25 °C are 105.6, 108.5, 116.0, 120.0 and

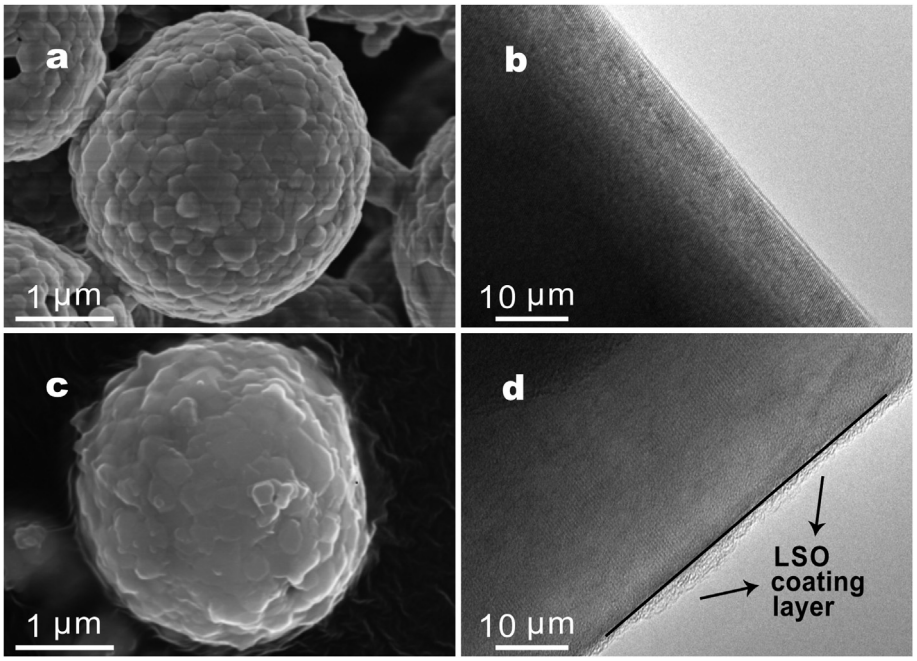

Fig. 6. SEM and TEM images of LNMO and LNMOF-LSO-2: (a) SEM and (b) TEM images of LNMO, (c) SEM and (d) TEM images of LNMOF-LSO-2.

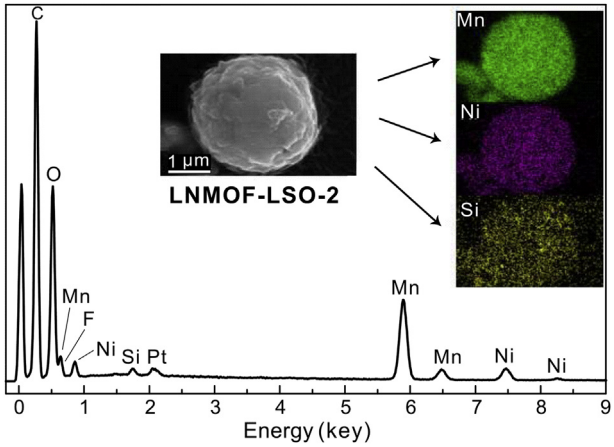

Fig. 7. EDS mappings of Mn, Ni and Si elements and electron probe micro analysis images for LNMOF-LSO-2 sample.

111.7 mA h g^{-1}. The discharge capacity retention of the five samples remain 92.6%, 94.1%, 95.2%, 97.8% and 97.3%. F doping and Li_4SiO_4 coating both are conducive to the improvement of the discharge capacity retention. Compared to the normal temperature (25 °C), the improvement at elevated temperature is more obvious. The discharge capacity retention of the five samples at 55 °C remain 54.9%, 82.4%, 88.4%, 94.2% and 93.7%.

Fig. 8c and e shows the rate capability curves at different rates (0.1 C–15 C) in the potential range of 3.5–5.0 V at 25 °C and 55 °C, respectively. At high rates (i.e., >1 C), the LNMOF sample exhibits a higher discharge capacity than the LNMO sample, and the LNMOF-LSO-2 sample exhibits the highest discharge capacity among the five samples. In addition, all of the five cathode materials have an excellent recovery capability.

Compared to the non-spherical $LiNi_{0.5}Mn_{1.5}O_4$ [6,10], the spherical particles have a better rate, mainly resulting from the special structure with porous surface and hollow inside [42–45]. The electrochemical performance of the samples is more superior than that of the cathode materials reported in other previous work [46–50]. The results indicate that F-doped and Li_4SiO_4 coating for $LiNi_{0.5}Mn_{1.5}O_4$ spinel are substantially effective for the enhancement of discharge capacity, capacity retention and rate capability during cycling. The ineffective performance of pristine $LiNi_{0.5}Mn_{1.5}O_4$ can be due to the dissolution of transition metals into the electrolyte and the oxidative decomposition of the electrolyte. F doping can ensure the crystal structure of $LiNi_{0.5}Mn_{1.5}O_4$ more stable. Li_4SiO_4 coating is effective in preventing transition metals from dissolving into the electrolyte as a protecting layer. Li_4SiO_4 coating can favor the improvement of the rate capability acting as an effective lithium ion conductor.

Fig. 8f shows the typical cyclic voltammogram curves of LNMO, LNMOF and LNMOF-LSO-2 conducted in the potential voltage range of 3.5–5 V at a sweep rate of 0.1 mV s^{-1}. The three samples show very similar CV curves. The CV curves of LNMOF-LSO-2 have higher and sharper peaks around 4.7 V (vs. Li/Li^+) than LNMO and LNMOF at 4.7 V (vs. Li/Li^+), indicating a higher greater discharge capacity. All of them the samples show a very weak peak around at 4 V (vs. Li/Li^+), which means the existence of the very small amount of Mn^{3+}. Moreover, compared to LNMO, a higher peak of LNMOF at 4 V demonstrates a greater amount of Mn^{3+} possessed by LNMOF. The result is consistent with the galvanostatic charge and discharge tests.

Fig. 9 shows the electrochemical impedance spectra of LNMO, LNMOF, LNMOF-LSO-1, LNMOF-LSO-2 and LNMOF-LSO-3 and corresponding fitting curves after 100th

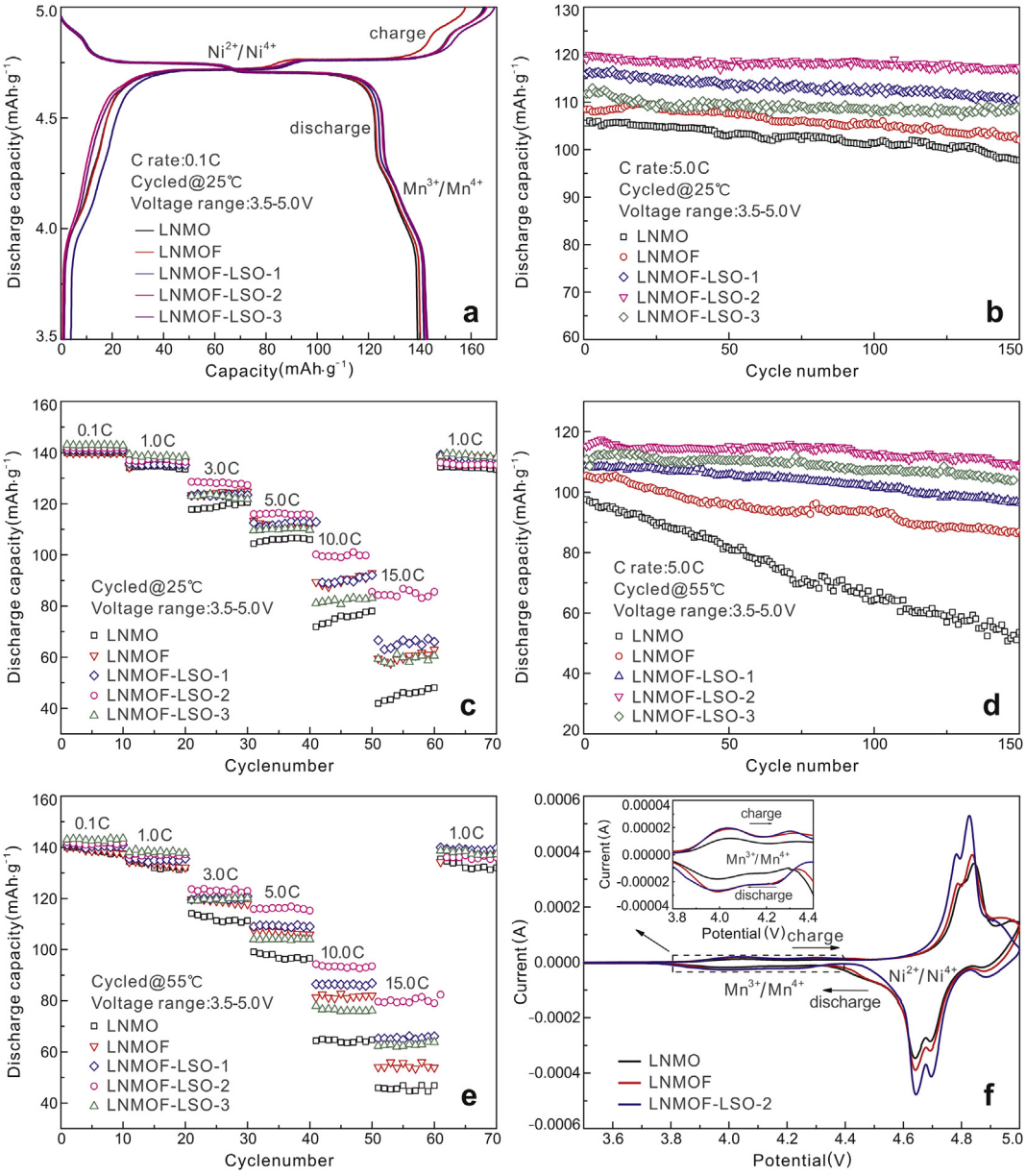

Fig. 8. (a) Charge and discharge curves of LNMO, LNMOF, LNMOF-LSO-1, LNMOF-LSO-2 and LNMOF-LSO-3; (b), (d) cycling performance of LNMO, LNMOF, LNMOF-LSO-1, LNMOF-LSO-2 and LNMOF-LSO-3 at 5 C, 25 °C and 55 °C; (c), (e) rate capacity at different rates from 0.1 C to 15 C at 25 °C and 55 °C; (f) cyclic voltammogram curves of the LNMO, LNMOF and LNMOF-LSO-2 samples.

cycle at 5 C and 55 °C, respectively. To better understand the role of F doping and Li_4SiO_4 coating, we performed electrochemical impedance spectroscopy analyses of the cells after 100 cycles at 55 °C. As showed in Fig. 9, a *Z*-view fitting procedure was used to simulate these Nyquist plots applying the inset equivalent circuit, all of the impedance spectra contain two semicircular curves and a line inclined at a constant angle. According to the literature H. Fang et al. [51], R_s represents the resistance of electrolyte solution; the high-frequency semicircle represents the resistance (R_{sf}) of solid-state interface layer formed on the surface of the electrodes; the intermediate-frequency semicircle represents the charge-transfer resistance (R_{ct}) in the electrode/electrolyte interface; and the slope in the low frequency represents the Warburg impedance (W_o) of lithium-ion diffusion in the bulk material. The R_{sf} values of the five samples are 167.7, 126.6, 84.17, 74.5 and 80.25 Ω, respectively. It can be seen that the doped samples (LNMOF) have lower interfacial layer resistance (R_{sf}) than the pristine sample (LNMO), which proves that the F doping is beneficial to favor the decrease of the formation of the solid-state interface layer during cycling. Compared with to the doped samples (LNMOF), the R_{sf} values of the coated samples (i.e., LNMOF-LSO-1, LNMOF-LSO-2 and LNMOF-LSO-3) decrease further, demonstrating that the Li_4SiO_4 coating is another an effective way to decrease the formation of the solid-state interface layer and suppress the reaction between the cathode surface and electrolyte during cycling. The R_{sf} value of LNMOF-LSO-2 is the lowest among those of

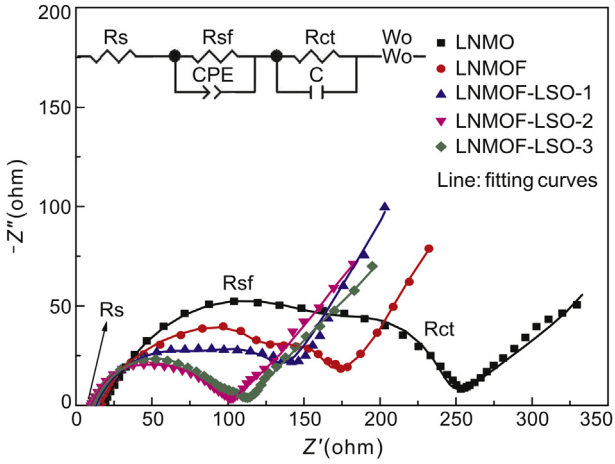

Fig. 9. Electrochemical impedance spectra of LNMO, LNMOF, LNMOF-LSO-1, LNMOF-LSO-2 and LNMOF-LSO-3 and corresponding fitting curves after 100th cycle at 5 C and 55 °C.

five samples, showing that 2 wt.% coating is an optimum amount, and the excessive coating hinders the improvement of performance. This result is consistent with the electrochemical performances of the five samples.

4. Conclusions

Spinel $LiNi_{0.5}Mn_{1.5}O_4$ microspheres were synthesized by a co-precipitation method. There were no impurity phases existing in this material based on the XRD analysis. F doping and Li_4SiO_4 coating were utilized to improve the electrochemical performance of spinel $LiNi_{0.5}Mn_{1.5}O_4$ cathode materials. F doping and Li_4SiO_4 coating did not change the crystal structure of the pristine $LiNi_{0.5}Mn_{1.5}O_4$ (space group $Fd\bar{3}m$). The role of doped F is to stabilize the spinel structure and so then to improve rate capability and cycle stability at room temperature. Coated Li_4SiO_4, acting as a protective layer and superionic conductor, further enhances rate capability and cycle stability at elevated temperatures. Moreover, $LiNi_{0.5}Mn_{1.5}O_{3.98}F_{0.02}$ coated with 2 wt.% Li_4SiO_4 exhibited the optimum electrochemical performance.

Acknowledgments

This work was supported by the National Natural Science Foundation of China (No. 51172124, 51372136) and Shenzhen Basic Research Project (No. JCYJ20130402145002372).

References

[1] Park OK, Cho Y, Lee S, Yoo HC, Song HK, Cho J. Who will drive electric vehicles, olivine or spinel? Energy Environ Sci 2011;4:1621–33.
[2] Liu Y, Zhang M, Xia Y, Qiu B, Liu Z, Li X. One-step hydrothermal method synthesis of core–shell $LiNi_{0.5}Mn_{1.5}O_4$ spinel cathodes for Li-ion batteries. J Power Sources 2014;256:66–71.
[3] Amine K, Tukamoto H, Yasuda H, Fujita Y. Preparation and electrochemical investigation of $LiMn_{2-x}Me_xO_4$ (Me: Ni, Fe, and $x = 0.5, 1$) cathode materials for secondary lithium batteries. J Power Sources 1997;68:604–8.
[4] Kim JH, Myung ST, Yoon CS, Kang SG, Sun YK. Comparative study of $LiNi_{0.5}Mn_{1.5}O_{4-\delta}$ and $LiNi_{0.5}Mn_{1.5}O_4$ cathodes having two crystallographic structures: $Fd\bar{3}m$ and $P4_332$. Chem Mater 2004;16:906–14.
[5] Jin YC, Lin CY, Duh JG. Improving rate capability of high potential $LiNi_{0.5}Mn_{1.5}O_{4-x}$ cathode materials via increasing oxygen non-stoichiometries. Electrochim Acta 2012;69:45–50.
[6] Hai B, Shukla AK, Duncan H, Chen G. The effect of particle surface facets on the kinetic properties of $LiMn_{1.5}Ni_{0.5}O_4$ cathode materials. J Mater Chem A 2013;1:759–69.
[7] Aurbach D, Markovsky B, Salitra G, Markevich E, Talyossef Y, Koltypin M, et al. Review on electrode–electrolyte solution interactions, related to cathode materials for Li-ion batteries. J Power Sources 2007;165:491–9.
[8] Yang L, Ravdel B, Lucht BL. Electrolyte reactions with the surface of high voltage $LiNi_{0.5}Mn_{1.5}O_4$ cathodes for lithium-ion batteries. Electrochem Solid-State Lett 2010;13:A95–7.
[9] Santhanam R, Rambabu B. Research progress in high voltage spinel $LiNi_{0.5}Mn_{1.5}O_4$ material. J Power Sources 2010;195:5442–51.
[10] Deng YF, Zhao SX, Xu YH, Nan CW. Effect of temperature of Li_2O–Al_2O_3–TiO_2–P_2O_5 solid-state electrolyte coating process on the performance of $LiNi_{0.5}Mn_{1.5}O_4$ cathode materials. J Power Sources 2015;296:261–7.
[11] Ito A, Li D, Lee Y, Kobayakawa K, Sato Y. Influence of Co substitution for Ni and Mn on the structural and electrochemical characteristics of $LiNi_{0.5}Mn_{1.5}O_4$. J Power Sources 2008;185:1429–33.
[12] Wang H, Xia H, Lai MO, Lu L. Enhancements of rate capability and cyclic performance of spinel $LiNi_{0.5}Mn_{1.5}O_4$ by trace Ru-doping. Electrochem Commun 2009;11:1539–42.
[13] Liu J, Manthiram A. Understanding the improved electrochemical performances of $LiNi_{0.5}Mn_{1.5}O_4$. J Phys Chem C 2009;113:15073–9.
[14] Chemelewski KR, Manthiram A. Origin of site disorder and oxygen nonstoichiometry in $LiMn_{1.5}Ni_{0.5-x}M_xO_4$ (M = Cu and Zn) cathodes with divalent dopant ions. J Phys Chem C 2013;117:12465–71.
[15] Locati C, Lafont U, Simonin L, Ooms F, Kelder EM. Mg-doped $LiNi_{0.5}Mn_{1.5}O_4$ spinel for cathode materials. J Power Sources 2007;174:847–51.
[16] Aklalouch M, Amarilla JM, Rojas RM, Saadoune I, Rojo JM. Chromium doping as a new approach to improve the cycling performance at high temperature of 5 V $LiNi_{0.5}Mn_{1.5}O_4$-based positive electrode. J Power Sources 2008;185:501–11.
[17] Xu XX, Yang J, Wang YQ, NuLi YN, Wang JL. $LiNi_{0.5}Mn_{1.5}O_{3.975}F_{0.05}$ as novel 5 V cathode material. J Power Sources 2007;174:1113–6.
[18] Sun YK, Oh SW, Yoon CS, Bang HJ, Prakash J. Effect of sulfur and nickel doping on morphology and electrochemical performance of $LiNi_{0.5}Mn_{1.5}O_{4-x}S_x$ spinel material in 3-V region. J Power Sources 2006;161:19–26.
[19] Kim WK, Han DW, Ryu WH, Lim SJ, Eom JY, Kwon HS. Effects of Cl doping on the structural and electrochemical properties of high voltage $LiNi_{0.5}Mn_{1.5}O_4$ cathode materials for Li-ion batteries. J Alloys Compd 2014;592:48–52.
[20] Oh SW, Park SH, Kim JH, Bae YC, Sun YK. Improvement of electrochemical properties of $LiNi_{0.5}Mn_{1.5}O_4$ spinel material by fluorine substitution. J Power Sources 2006;157:464–70.
[21] Sun YK, Hong KJ, Prakash J, Amine K. Electrochemical performance of nano-sized ZnO-coated $LiNi_{0.5}Mn_{1.5}O_4$ spinel as 5 V materials at elevated temperatures. Electrochem Commun 2002;4:344–8.
[22] Wu HM, Belharouak I, Abouimrane A, Sun YK, Amine K. Surface modification of $LiNi_{0.5}Mn_{1.5}O_4$ by ZrP_2O_7 and ZrO_2 for lithium-ion batteries. J Power Sources 2010;195:2909–13.
[23] Wang Y, Peng Q, Yang G, Yang Z, Zhang L, Long H, et al. High-stability 5 V spinel $LiNi_{0.5}Mn_{1.5}O_4$ sputtered thin film electrodes by modifying with aluminium oxide. Electrochim Acta 2014;136:450–6.
[24] Kang HB, Myung ST, Amine K, Lee SM, Sun YK. Improved electrochemical properties of BiOF-coated 5 V spinel $LiNi_{0.5}Mn_{1.5}O_4$ for rechargeable lithium batteries. J Power Sources 2010;195:2023–8.
[25] Shi JY, Yi CW, Kim K. Improved electrochemical performance of $AlPO_4$-coated $LiNi_{0.5}Mn_{1.5}O_4$ electrode for lithium-ion batteries. J Power Sources 2010;195:6860–6.

[26] Hu DH, Zhao SX, Deng YF, Nan CW. Synthesis and electrochemical performance of rod-like spinel $LiMn_2O_4$ coated by Li–Al–Si–O solid electrolyte. J Mater Chem A 2013;1:14729–35.
[27] Deng YF, Zhao SX, Xu YH, Nan CW. Effect of the morphology of Li–La–Zr–O solid electrolyte coating on the electrochemical performance of spinel $LiMn_{1.95}Ni_{0.05}O_{3.98}F_{0.02}$ cathode materials. J Mater Chem A 2014;2:18889–97.
[28] Deng YF, Zhao SX, Hu DH, Nan CW. Structure and electrochemical performance of spinel $LiMn_{1.95}Ni_{0.05}O_{3.98}F_{0.02}$ coated with Li–La–Zr–O solid electrolyte. J Solid State Electrochem 2013;18:249–55.
[29] Sakuda A, Kitaura H, Hayashi A, Tadanaga K, Tatsumisago M. Improvement of high-rate performance of all-solid-state lithium secondary batteries using $LiCoO_2$ coated with Li_2O–SiO_2. Electrochem Solid-State Lett 2008;11:A1–3.
[30] Zhao E, Liu X, Zhao H, Xiao X, Hu Z. Ion conducting Li_2SiO_3-coated lithium-rich layered oxide exhibiting high rate capability and low polarization. Chem Commun 2015;51:9093–6.
[31] Raistrick ID, Ho C, Huggins RA. Ionic-conductivity of some lithium silicates and aluminosilicates. J Electrochem Soc 1976;123:1469–76.
[32] West AR, Glasser FP. Crystallisation of lithium zinc silicates. 2. Comparison of metastable phase relations and properties of lithium zinc orthosilicates. J Mater Sci 1970;5:676–88.
[33] West AR. Ionic conductivity of oxides based on Li_4SiO_4. J Appl Electrochem 1973;3:327–35.
[34] Zhang Q, Jiang W, Zhou Z, Wang S, Guo X, Zhao S, et al. Enhanced electrochemical performance of Li_4SiO_4-coated $LiFePO_4$ prepared by sol–gel method and microwave heating. Solid State Ionics 2012;218:31–4.
[35] Adnan SBRS, Mohamed NS. Citrate sol–gel synthesised Li_4SiO_4: conductivity and dielectric behaviour. Mater Res Innov 2012;16:281–5.
[36] Wang H, Shi Z, Li J, Yang S, Ren R, Cui J, et al. Direct carbon coating at high temperature on $LiNi_{0.5}Mn_{1.5}O_4$ cathode: Unexpected influence on crystal structure and electrochemical performances. J Power Sources 2015;288:206–13.
[37] Wang G, Xie J, Zhu T, Cao G, Zhao X, Zhang S. Self-templating synthesis of single crystalline $LiNi_{0.5}Mn_{1.5}O_4$ nanotubes with improved electrochemical performance. Funct Mater Lett 2014;07:1450009.
[38] Tang ZY, Lu XH, Zhang N. The anion-cation multiple doping effect of spinel cathode materials on electrochemical speciality. Acta Phys Chim Sin 2005;21:934–8.
[39] Amdouni N, Zaghib K, Gendron F, Mauger A, Julien CM. Structure and insertion properties of disordered and ordered $LiNi_{0.5}Mn_{1.5}O_4$ spinels prepared by wet chemistry. Ionics 2006;12:117–26.
[40] Liu G, Park KS, Song J, Goodenough JB. Influence of thermal history on the electrochemical properties of $LiNi_{0.5}Mn_{1.5}O_4$. J Power Sources 2013;243:260–6.
[41] Xue Y, Wang Z, Yu F, Zhang Y, Yin G. Ethanol-assisted hydrothermal synthesis of $LiNi_{0.5}Mn_{1.5}O_4$ with excellent long-term cyclability at high rate for lithium-ion batteries. J Mater Chem A 2014;2:4185–91.
[42] Liu J, Xia H, Lu L, Xue DF. Anisotropic Co_3O_4 porous nanocapsules toward high-capacity Li-ion batteries. J Mater Chem 2010;20:1506–10.
[43] Liu J, Liu F, Gao K, Wu J, Xue DF. Recent developments in the chemical synthesis of inorganic porous capsules. J Mater Chem 2009;19:6073–84.
[44] Liu J, Xue D. Thermal oxidation strategy towards porous metal oxide hollow architectures. Adv Mater 2008;20:2622–7.
[45] Cui Y, Wang J, Wang M, Zhuang Q. Electrochemical performance and electronic properties of shell $LiNi_{0.5}Mn_{1.5}O_4$ hollow spheres for lithium ion battery. Funct Mater Lett 2016. http://dx.doi.org/10.1142/S1793604716500272.
[46] Liu W, Liu J, Chen K, Ji S, Wan Y, Zhou Y, et al. Enhancing the electrochemical performance of the $LiMn_2O_4$ hollow microsphere cathode with a $LiNi_{0.5}Mn_{1.5}O_4$ coated layer. Chem Eur J 2014;20:824–30.
[47] Chen KF, Donahoe AC, Noh YD, Li KY, Komarneni S, Xue DF. Conventional- and microwave-hydrothermal synthesis of $LiMn_2O_4$: effect of synthesis on electrochemical energy storage performances. Ceram Int 2014;40:3155–63.
[48] Chen KF, Xue DF. Anode performances of mixed $LiMn_2O_4$ and carbon black toward lithium-ion battery. Funct Mater Lett 2014;07:1450017.
[49] Li K, Lin S, Shua F, Zhang J, Chen KF, Xue DF. A rapid combustion route to synthesize high-performance nanocrystalline cathode materials for Li-ion batteries. CrystEngComm 2014;16:10969–76.
[50] Zhang JW, Lin SD, Li KY, Shua FF, Chen KF, Wang LQ, et al. Synthesis of spinel $LiMn_2O_4$ cathode material by a modified solid state reaction. Funct Mater Lett 2015;08:1540002.
[51] Fang H, Wang Z, Zhang B, Li X, Li G. High performance $LiNi_{0.5}Mn_{1.5}O_4$ cathode materials synthesized by a combinational annealing method. Electrochem Commun 2007;9:1077–82.

Dr. Shi-Xi Zhao is an associate professor at Graduate Shool at Shenzhen, Tsinghua University. He received his Ph.D. (2002) in materials science from Wuhan University of Technology. From 2002 to 2004, he engaged in postdoctoral research at Department of Chemistry, Tsinghua University. He has worked at Graduate School at Shenzhen, Tsinghua University since Aug. 2004. His current research is focused mainly on Li-ion battery and supercapacitor materials, and functional ceramics. He has published over fifty academic papers and holds six Chinese patents.